encit 2020

ABCM Associação Brasileira de Engenharia e Ciências Mecânicas

18th Brazilian Congress of Thermal Sciences and Engineering
November 16–20, 2020 (Online)

ENC-2020-0350
A Detailed Approach for the Classical Integral Transform Technique in Ablation Phenomenon with Moving Boundaries

Gilvan do Nascimento Filho
Jakler Nichele
Military Institute of Engineering (IME)
contato.gfilho@gmail.com
jakler.ime@gmail.com

Leonardo Santos de Brito Alves
Fluminense Federal University (UFF)
leonardo.alves@gmail.com

Abstract. *The ablation phenomenon is present in several applications, such as hypersonic rockets and ballistic missiles, atmospheric reentry vehicles, and rocket nozzles. Ablation is also considered as a Thermal Protection System (TPS), along with heat sinks, cooling, and surface insulation, however, the difference is that in ablation the material is expended to absorb thermal energy and therefore prevents damage to the vehicle and its components. The objective of the present study is to simulate this physical phenomenon computationally, evaluating the thermal profile of the ablative material when submitted to hypersonic flow. For this simulation, the Classical Integral Transform Technique (CITT) is used to obtain the analytical solution of the governing equation that rules the ablative phenomenon, considering a constant heat flux throughout the process. Herein, the non-homogeneity of the boundary conditions, present in the set of equations that govern the phenomenon, is expected to expand the system perturbation and create an oscillation. Therefore, in order to minimize the perturbation, new variables must be considered in the govern equation homogenizing the boundary conditions and eliminating the oscillation.*

Keywords: *Ablation, Classical Integral Transform Technique, Heat Transfer, Ablative Material, Parabolic PDE*

1. INTRODUCTION

Ablative materials are used in thermal protection systems to both cool and protect mechanical structures exposed to extremely high temperatures, such as hypersonic rockets and ballistic missiles, atmospheric reentry vehicles and rocket nozzles. They are designed to burn slowly in a controlled manner, so that heat can be removed by the gases generated, whereas the remaining solid material insulates the spacecraft from superheated gases (Sundén and Fu, 2017). Ablation phenomenon is among the moving-boundary or phase-change problems, for which heat transfer is coupled with the melting and chemical decomposition of the material (Hahn and Özişik, 2012).

The ablative materials are divided into two categories: melting (thermoplastics) and non-melting. The non-melting category are divided into two classes: high-temperature ablators (HTA – carbon/carbon and carbon/silicon carbide ceramic matrix composites) and low-temperature ablators (LTA - thermosetts). The LTAs are made of char-forming plastics, which provide multiple levels of protection by introducing pyrolysis gases. The gas formation, which is chemically reacting with the char, blocks the heat propagation and slows down the melting of the ablative material. It happens because a lot of heat is consumed during the decomposition of the thermosetts. The HTAs has three-dimensional C – C composites and are used in nose tip and leading edges. Because of their excellent strength retention with increase in temperature, the material remains in place and blocks the heat for longer duration and, subsequently, gets removed by oxidation at higher temperatures (Palaninathan and Bindu, 2005).

Ablation has been studied since the 1950s and 1960s, and at that time, ablation in a rocket engine was addressed by dividing the analytical solution into two time periods: first where material undergoes heating to an ablation point, and a second period in which the ablative material is consumed to decrease the rate of heat transfer. Thermal diffusivity is considered in the porous region of the char layer in an environment with the presence of gas release (Chen, 1965).

As time passed, new techniques for ablation have been developed. One of them is by approximating the system of PDEs through the elimination of the spatial dependence of the system, i.e., the trapezoidal rule for integration eliminates the spatial component and the mathematical model of the physical phenomenon consists only of its temporal component (Ruperti Jr. *et al.*, 2004).

Another way of modeling the ablation is in which the inverse problem is solved through the minimization of functional, for the no-ablation and the ablation time period, which are optimized by a method of iterative step search (Oliveira and Orlande, 2004).

With new techniques for solving the phenomenon, the method robustness needed further enhancing, i.e., new parameters were added to the problem in order to improve its application. So, the inclusion of radiation to the ablative model alters the government equation of the phenomenon, which is solved via GITT. Besides that, the heat transfer rate follows a second order polynomial model as a function of time (Gomes *et al.*, 2005).

Moreover, the approach could be taken by considering a generalization of the coordinates for different geometries and the dimensionless temperature variable changed in order to homogenize the boundary conditions (Gomes *et al.*, 2006).

The inclusion of radiation, which alters the government equation to a hyperbolic PDE, was analyzed via GITT, resulting in a system of some ordinary second order differential equations in the time variable. With the transformation of the government equation, the problem is analyzed numerically for different Biot numbers. Biot numbers represents the ratio of conduction resistance within the body to convection resistance at the surface of the body (Monteiro *et al.*, 2009).

Instead of using the aforementioned approaches, one could analyze the ablative phenomenon aerothermodynamically using Navier-Stokes as the government equation. The problem is approached in two dimensions to assess how the phenomenon occurs in the area of a spherical cylinder and the ablation analysis is carried out using the Enthalpy Method Candane *et al.* (2009).

Bianchi (2007) includes an analytical and numerical analysis, in addition to modeling the phenomenon via CFD. Analytically, the author performs energy and mass balances on the surface, as well as analyzing thermochemically the physical problem to predict the ablation rate. Numerically, it is used Crank-Nicholson Method to achieve solution.

However, not only the heat transfer in ablation must be investigated. It is of fundamental importance to assess the physical aspects of the materials used as TPS, which are analyzed by the deformation and stress present in the ablative material when occurring a surface recession (Palaninathan and Bindu, 2005).

The present study employs the Classical Integral Transform Technique (CITT) to obtain the thermal profile in the ablative material during its burning. To solve the problem a simplified mathematical model was used, in which a constant heat flux replaced the effects of the aerodynamic heating imposed by the external flow. It is clarified the oscillation problem generated by the non-homogeneity of the boundary conditions when applying CITT to solve the problem. Furthermore, well known dimensionless variables which homogenize the boundary conditions are taken into account in-depth. This is an important consideration when comparing results from various studies for the ablation phenomenon. Finally, since the study was generically developed, one can calculate the aerodynamic heat and include it to the solution here presented. Despite of that, this initial approach to the phenomenon develops a ground base for the inclusion of the pyrolysis heat into the ablation phase problem, by taking into account the compound of a graphite ablator (LTA), which releases several gaseous products for the in-depth chemical reactions of pyrolysis.

2. THEORETICAL FUNDAMENTALS

The mathematical analysis of the ablation dynamics is structured in two phases: no-ablation and ablation. In the no-ablation phase, the slab with initial temperature $\theta(\eta, 0)$ will be heated until it reaches the phase-change temperature $\theta(0, \tau_0) = 1$. Otherwise, in the ablation the problem itself is readily obtained from the solution of the heat conduction problem at time τ_0 (Ruperti Jr. *et al.*, 2004).

For this formulation, it is assumed that radiation effects can be neglected and, thereby, convective effects prevail on the heat flux. Thus, the govern equation stands for a parabolic PDE. The radiation effects become relevant when the flow velocity is greater than 10 km/s.

The one dimensional, time dependent heat-conduction problem in no-ablation time period (Fig. 1) is given by

$$\begin{cases} \dfrac{\partial \theta(\eta,\tau)_{nab}}{\partial \tau} = \dfrac{\partial^2 \theta(\eta,\tau)_{nab}}{\partial \eta^2}, \quad 0 \le \eta \le 1 \quad \text{e} \quad 0 \le \tau \le \tau_0 & \text{(1a)} \\ \theta(\eta,0)_{nab} = 0, \quad 0 \le \eta \le 1 \quad \text{e} \quad \tau = 0 & \text{(1b)} \\ -\dfrac{\partial \theta(0,\tau)_{nab}}{\partial \eta} = Q(\tau), \quad \eta = 0 \quad \text{e} \quad 0 \le \tau \le \tau_0 & \text{(1c)} \\ \dfrac{\partial \theta(1,\tau)_{nab}}{\partial \eta} = 0, \quad \eta = 1 \quad \text{e} \quad 0 \le \tau \le \tau_0 & \text{(1d)} \end{cases}$$

where θ is the dimensionless temperature profile of the ablative material, η the dimensionless position of the slab, τ corresponds to the dimensionless time, τ_0 is the time period of phase transition and $Q(\tau)$ is the dimensionless heat flux (Chen, 1965; Ruperti Jr. *et al.*, 2004; Oliveira and Orlande, 2004; Gomes *et al.*, 2005, 2006; Monteiro *et al.*, 2009; Sias, 2009). These variables are defined as

$$\theta(\eta,\tau) = \frac{T(x,t) - T_0}{T_{ab} - T_0} \tag{2}$$

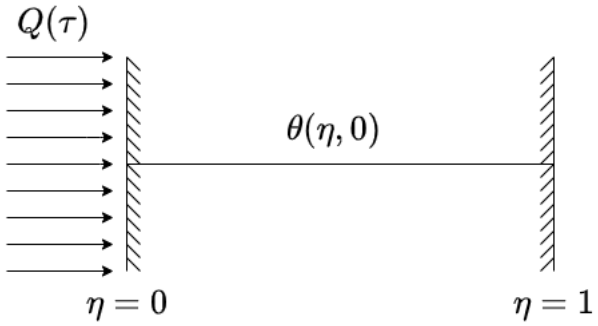

Figure 1: Schematic diagram of the initial and boundary conditions of the ablative material subject to a heat flux $Q(\tau)$ at $\eta = 0$.

$$\eta = \frac{x}{L} \tag{3}$$

$$\tau = \frac{\alpha}{L^2} t \tag{4}$$

$$Q(\tau) = \frac{Lq}{k(T_{ab} - T_0)} \tag{5}$$

where $T(x,t)$ is the temperature profile of the ablative material, T_0 corresponds to the initial temperature of the slab, T_{ab} denotes the phase-change temperature, x is the spatial coordinate, t denotes time, L is thickness of the protective layer, α is the thermal diffusivity, q denotes the heat flux and k is the thermal conductivity.

Now, the one dimensional, time dependent heat-conduction ablation phase problem is given by

$$\begin{cases} \dfrac{\partial \theta(\eta,\tau)_{ab}}{\partial \tau} = \dfrac{\partial^2 \theta(\eta,\tau)_{ab}}{\partial \eta^2}, \quad S(\tau) \leq \eta \leq 1 \quad \text{e} \quad \tau \geq \tau_0 & \text{(6a)} \\ \theta(\eta,\tau_0)_{ab} = \theta_0(\eta)_{nab}, \quad S(\tau) \leq \eta \leq 1 \quad \text{e} \quad \tau = \tau_0 & \text{(6b)} \\ \theta(S(\tau),\tau)_{ab} = 1, \quad \eta = S(\tau) \quad \text{e} \quad \tau \geq \tau_0 & \text{(6c)} \\ \dfrac{\partial \theta(1,\tau)_{ab}}{\partial \eta} = 0, \quad \eta = 1 \quad \text{e} \quad \tau \geq \tau_0 & \text{(6d)} \end{cases}$$

The energy balance in $\eta = S(\tau)$ gives the phase-change in space, i.e.,

$$\frac{1}{\text{Ste}} \frac{dS(\tau)}{d\tau} = Q(\tau) + \frac{\partial \theta(S(\tau),\tau)}{\partial \eta}, \quad \tau \geq \tau_0 \tag{7}$$

where $S(\tau)$ is the dimensionless space position where the ablation takes place and *Ste* corresponds to the Stefan number, which is used to describe the ratio between the sensible heat and the latent heat of ablation, H. The c_p in Eq. 8 denotes the specific heat.

$$\text{Ste} = \frac{c_p(T_{ab} - T_0)}{H} \tag{8}$$

3. METHODOLOGY

3.1 Classical Integral Transform Technique

Here, TEFLON was chosen as the ablative material. It will be sublimated and removed from the body by the external flow. Table 1 presents the properties of the TEFLON, (Ruperti Jr. *et al.*, 2004). It was assumed a constant heat flux q throughout the total time of exposition of the body to the hypersonic flow, which its value corresponds to a mean heat flux seen in the literature. This assumption gives a simpler approach when applying the CITT to obtain the temperature profile of the 1D slab. The value of the net heat flux, here considered, stands for an hypersonic flow, however the flow velocity is not greater than 10 km/s. In this way, the hypothesis of neglecting the effects of radiation is reasonable and the problem can be described as a parabolic partial differential equation.

By applying CITT (Hahn and Özişik, 2012) in no-ablation problem (Eq. 1), it is possible to obtain

$$\theta(\eta,\tau)_{nab} = \sum_{i=1}^{\infty} \frac{1}{N_i} \cos(\beta_i \eta) e^{(-\alpha \beta_i^2 \tau)} \left[\int_0^{\tau} Q(\tau) e^{(\alpha \beta_i^2 \tau)} d\tau \right] \tag{9}$$

Table 1: TEFLON properties.

Variable	Value	Unity
L	0.0065	m
k	0.22	W/(m·K)
α	0.00929	m^2/s
q	100	W/m^2
c_p	1256	J/(kg·K)
H	2326	kJ/kg
T_{ab}	833	K
T_o	416	K

where β_i and N_i are the eigenvalues and the norms of the eigenfunction, respectively,

$$\beta_i = i \cdot \pi, \quad i = 1, 2, 3... \tag{10}$$

$$\begin{cases} \dfrac{1}{N_i} = \dfrac{2}{L}, & \beta_i \neq 0 \quad (11a) \\ \dfrac{1}{N_i} = \dfrac{1}{L}, & \beta_i = 0 \quad (11b) \end{cases}$$

For the ablation problem (Eq. 6), the dimensionless temperature profile of the slab is described as

$$\theta(\eta, \tau)_{ab} = \sum_{i=1}^{\infty} \frac{1}{N_i} \sin(\beta_i \eta) e^{(-\alpha \beta_i^2 \tau)} \left[\int_{S(\tau)}^{1} \sin(\beta_i \eta) \theta_0 d\eta + \int_{\tau_0}^{\tau} \frac{d \sin(\beta_i S(\tau))}{d\eta} e^{(\alpha \beta_i^2 \tau)} d\tau \right] \tag{12}$$

where θ_0 is the dimensionless temperature profile of the slab at the start of the ablation time period, computed with Eq. 9, and β_i and N_i are now given by

$$\beta_i = \frac{i \cdot \pi}{2}, \quad i = 1, 2, 3... \tag{13}$$

$$\frac{1}{N_i} = \frac{2}{L} \tag{14}$$

The phase-change energy balance (Eq. 7) can be solved using the second order Runge-Kutta (Tannehill *et al.*, 1997) method. With this solution, the dimensionless space position where ablation occurs is determined.

$$S_\eta^{\tau+1} = S_\eta^\tau + q_\eta^{(2)} \tag{15}$$

$$q_\eta^{(2)} = \Delta t \left[\frac{1}{\mathrm{Ste}} \left(Q(\tau) + \frac{\theta_{\eta+1}^\tau - \theta_\eta^\tau}{\Delta \eta} + \frac{1}{2} q_\eta^{(1)} \right) \right] \tag{16}$$

$$q_\eta^{(1)} = \Delta t \left[\frac{1}{\mathrm{Ste}} \left(Q(\tau) + \frac{\theta_{\eta+1}^{\tau-1} - \theta_\eta^{\tau-1}}{\Delta \eta} \right) \right] \tag{17}$$

3.2 Homogenization of the Boundary Conditions for CITT Application

The non-homogeneity present in the boundary conditions creates an oscillatory profile for the solution which is not real (Marchenko and Khruslov, 2006; Pavliotis and Stuart, 2008). Therefore, in order to minimize these oscillations, new variables must be considered in the govern equation homogenizing the boundary conditions.

3.2.1 No-ablation time period with homogenized boundary conditions

It is represented in the literature that the heat flux occurs at $\eta = 1$, which was not used in the previous formulation. The position for the heat flux at $\eta = 1$ accounts the creation of new variables in order to homogenize Eq. 1c. This happens for one reason: to take into account the dimensionless space position for the creation of a new variable and, by doing so, the derivative terms in the boundaries can be represented as null, i.e., homogeneous.

Thereby, the heat flux now occurs at $\eta = 1$ (Fig. 2). Thus, the set of equations that govern the phenomenon in the no-ablation time period (Eq. 1) becomes

$$\begin{cases} \dfrac{\partial\theta(\eta,\tau)_{nab}}{\partial\tau} = \dfrac{\partial^2\theta(\eta,\tau)_{nab}}{\partial\eta^2}, \quad 0 \leq \eta \leq 1 \quad \text{e} \quad 0 \leq \tau \leq \tau_0 & \text{(18a)} \\ \theta(\eta,0)_{nab} = 0, \quad 0 \leq \eta \leq 1 \quad \text{e} \quad \tau = 0 & \text{(18b)} \\ \dfrac{\partial\theta(0,\tau)_{nab}}{\partial\eta} = 0, \quad \eta = 0 \quad \text{e} \quad 0 \leq \tau \leq \tau_0 & \text{(18c)} \\ -\dfrac{\partial\theta(1,\tau)_{nab}}{\partial\eta} = Q(\tau), \quad \eta = 1 \quad \text{e} \quad 0 \leq \tau \leq \tau_0 & \text{(18d)} \end{cases}$$

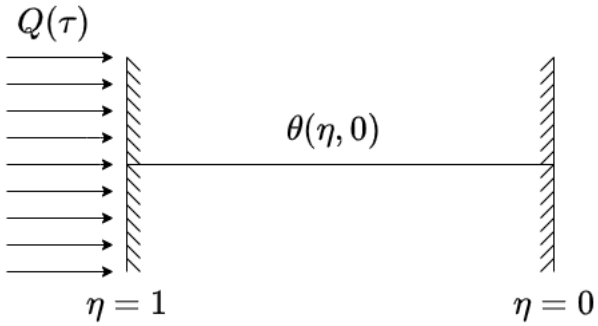

Figure 2: Schematic diagram of the initial and boundary conditions of the ablative material subject to a heat flux $Q(\tau)$ at $\eta = 1$.

The previous equations can be rewritten using the well-known dimensionless variables (Gomes *et al.*, 2006), given by

$$\theta^*(\eta,\tau)_{nab} = \theta(\eta,\tau)_{nab} + \left(\frac{\eta^2}{2}\right)\cdot Q(\tau) \tag{19}$$

To verify the homogenization at the boundaries, one must take the derivative of Eq. 19 with respect to η, which gives

$$\eta = 0: \quad \frac{\partial\theta^*(0,\tau)_{nab}}{\partial\eta} = \frac{\partial\theta(0,\tau)_{nab}}{\partial\eta} + [\eta\cdot Q(\tau)]_{(\eta=0)} = 0 \tag{20}$$

$$\eta = 1: \quad \frac{\partial\theta^*(1,\tau)_{nab}}{\partial\eta} = \frac{\partial\theta(1,\tau)_{nab}}{\partial\eta} + [\eta\cdot Q(\tau)]_{(\eta=1)} = -Q(\tau) + Q(\tau) = 0 \tag{21}$$

Substituting Eq. 18b into 19, in order to obtain the initial condition, leads to

$$\tau = 0: \quad \theta^*(\eta,0)_{nab} = \theta(\eta,0)_{nab} + \left(\frac{\eta^2}{2}\right)\cdot Q(0) = \left(\frac{\eta^2}{2}\right)\cdot Q(0) \tag{22}$$

Taking the derivative of Eq. 19 with respect to τ and η, to substitute afterwards in the govern equation (Eq. 18a)

$$\begin{cases} \dfrac{\partial\theta^*(\eta,\tau)_{nab}}{\partial\tau} = \dfrac{\partial\theta(\eta,\tau)_{nab}}{\partial\tau} + \left(\dfrac{\eta^2}{2}\right)\cdot\dfrac{dQ(\tau)}{d\tau} & \text{(23a)} \\ \dfrac{\partial\theta^*(\eta,\tau)_{nab}}{\partial\eta} = \dfrac{\partial\theta(\eta,\tau)_{nab}}{\partial\eta} + [\eta\cdot Q(\tau)] & \text{(23b)} \\ \dfrac{\partial^2\theta^*(\eta,\tau)_{nab}}{\partial\eta^2} = \dfrac{\partial^2\theta(\eta,\tau)_{nab}}{\partial\eta^2} + Q(\tau) & \text{(23c)} \end{cases}$$

By rearranging Eq. 23a and 23c and replacing them into Eq. 18a, the mathematical problem is established as

$$\begin{cases} \dfrac{\partial\theta^*(\eta,\tau)_{nab}}{\partial\tau} = \dfrac{\partial^2\theta^*(\eta,\tau)_{nab}}{\partial\eta^2} + \left(\dfrac{\eta^2}{2}\right)\cdot\dfrac{dQ(\tau)}{d\tau} - Q(\tau), \quad 0 \leq \eta \leq 1 \quad \text{e} \quad 0 \leq \tau \leq \tau_0 & \text{(24a)} \\ \theta^*(\eta,0)_{nab} = \left(\dfrac{\eta^2}{2}\right)\cdot Q(0), \quad 0 \leq \eta \leq 1 \quad \text{e} \quad \tau = 0 & \text{(24b)} \\ \dfrac{\partial\theta^*(0,\tau)_{nab}}{\partial\eta} = 0, \quad \eta = 0 \quad \text{e} \quad 0 \leq \tau \leq \tau_0 & \text{(24c)} \\ \dfrac{\partial\theta^*(1,\tau)_{nab}}{\partial\eta} = 0, \quad \eta = 1 \quad \text{e} \quad 0 \leq \tau \leq \tau_0 & \text{(24d)} \end{cases}$$

The CITT solution (Hahn and Özişik, 2012) for the the no-ablation problem (Eq. 24) results in

$$\theta^*(\eta,\tau)_{nab} = \sum_{i=1}^{\infty} \frac{1}{N_i}\cos(\beta_i\eta)e^{(-\alpha\beta_i^2\tau)} \cdot \left[\int_0^1 \cos(\beta_i\eta)\cdot\left(\frac{\eta^2}{2}\right)\cdot Q(\tau)d\eta + \right. \\ \left. \int_0^\tau \left(\int_0^1 \cos(\beta_i\eta)\cdot\left(\frac{\eta^2}{2}\right)\cdot\frac{dQ(\tau)}{d\tau}d\eta - \int_0^1 \cos(\beta_i\eta)\cdot Q(\tau)d\eta\right)e^{(\alpha\beta_i^2\tau)}d\tau\right] \tag{25}$$

with β_i and N_i being

$$\beta_i = i\cdot\pi, \quad i = 1,2,3... \tag{26}$$

$$\begin{cases} \dfrac{1}{N_i} = \dfrac{2}{L}, & \beta_i \neq 0 \quad (27a) \\ \dfrac{1}{N_i} = \dfrac{1}{L}, & \beta_i = 0 \quad (27b) \end{cases}$$

3.2.2 Ablation time period with homogenized boundary conditions

Following the same criteria presented in Section 3.2.1 changing the boundary position for the heat flux, the ablation phase problem (Eq. 6) is

$$\begin{cases} \dfrac{\partial\theta(\eta,\tau)_{ab}}{\partial\tau} = \dfrac{\partial^2\theta(\eta,\tau)_{ab}}{\partial\eta^2}, \quad 0\leq\eta\leq S(\tau) \quad \text{e} \quad \tau\geq\tau_0 & (28a) \\ \theta(\eta,\tau_0)_{ab} = \theta_0(\eta)_{nab}, \quad 0\leq\eta\leq S(\tau) \quad \text{e} \quad \tau=\tau_0 & (28b) \\ \dfrac{\partial\theta(0,\tau)_{ab}}{\partial\eta} = 0, \quad \eta = 0 \quad \text{e} \quad \tau\geq\tau_0 & (28c) \\ \theta(S(\tau),\tau)_{ab} = 1, \quad \eta = S(\tau) \quad \text{e} \quad \tau\geq\tau_0 & (28d) \end{cases}$$

The previous equations can be rewritten using the well-known dimensionless variables (Cotta and Mikhailov, 1993)

$$\theta^*(\eta,\tau^*)_{ab} = \theta(\eta,\tau)_{nab} - 1 \tag{29}$$

$$\tau^* = \tau - \tau_0 \tag{30}$$

To verify the homogenization at the boundaries, one must take the derivative of Eq. 29 with respect to η at $\eta = 0$ and assessing it at $\eta = S(\tau)$, i.e.

$$\eta = 0: \quad \frac{\partial\theta^*(0,\tau)_{ab}}{\partial\eta} = \frac{\partial\theta(0,\tau)_{ab}}{\partial\eta} = 0 \tag{31}$$

$$\eta = S(\tau): \quad \theta^*(S(\tau),\tau)_{ab} = \theta(S(\tau),\tau)_{ab} - 1 = 1 - 1 = 0 \tag{32}$$

The replacement of Eq. 28b into Eq. 29, in order to obtain the initial condition, leads to

$$\tau^* = 0: \quad \theta^*(\eta,0)_{ab} = \theta(\eta,\tau_0)_{ab} - 1 = \theta_0(\eta)_{nab} - 1 \tag{33}$$

The derivative of Eq. 29 with respect to τ and η, and substituting in the govern equation (Eq. 28a) leads to

$$\begin{cases} \dfrac{\partial\theta(\eta,\tau)_{ab}}{\partial\tau} = \dfrac{\partial\theta(\eta,\tau)_{ab}}{\partial\theta^*(\eta,\tau^*)_{ab}}\cdot\dfrac{\partial\theta^*(\eta,\tau^*)_{ab}}{\partial\tau^*}\cdot\dfrac{\partial\tau^*}{\partial\tau} = \dfrac{\partial\theta^*(\eta,\tau)_{ab}}{\partial\tau^*} & (34a) \\ \dfrac{\partial\theta(\eta,\tau)_{ab}}{\partial\eta} = \dfrac{\partial\theta(\eta,\tau)_{ab}}{\partial\theta^*(\eta,\tau^*)_{ab}}\cdot\dfrac{\partial\theta^*(\eta,\tau^*)_{ab}}{\partial\eta} = \dfrac{\partial\theta^*(\eta,\tau^*)_{ab}}{\partial\eta} & (34b) \\ \dfrac{\partial^2\theta^*(\eta,\tau^*)_{ab}}{\partial\eta^2} = \dfrac{\partial^2\theta(\eta,\tau)_{ab}}{\partial\eta^2} & (34c) \end{cases}$$

By rearranging Eq. 34a and 34c and replacing them into Eq. 28a, the new problem is established as

$$\begin{cases} \dfrac{\partial\theta^*(\eta,\tau^*)_{ab}}{\partial\tau^*} = \dfrac{\partial^2\theta^*(\eta,\tau^*)_{ab}}{\partial\eta^2}, \quad 0\leq\eta\leq S(\tau) \quad \text{e} \quad \tau^*\geq 0 & (35a) \\ \theta^*(\eta,0)_{ab} = \theta_0(\eta)_{nab} - 1, \quad 0\leq\eta\leq S(\tau) \quad \text{e} \quad \tau^* = 0 & (35b) \\ \dfrac{\partial\theta^*(0,\tau^*)_{ab}}{\partial\eta} = 0, \quad \eta = 0 \quad \text{e} \quad \tau^*\geq 0 & (35c) \\ \theta^*(S(\tau),\tau^*)_{ab} = 0, \quad \eta = S(\tau) \quad \text{e} \quad \tau^*\geq 0 & (35d) \end{cases}$$

The solution of the ablation phase problem obtained with CITT (Hahn and Özişik, 2012) in the set of equations that govern the phenomenon in the ablation time period (Eq. 35) is given by

$$\theta^*(\eta,\tau^*)_{ab} = \sum_{i=1}^{\infty} \frac{1}{N_i} \sin(\beta_i \eta) e^{(-\alpha\beta_i^2\tau)} \cdot \left[\int_0^1 \sin(\beta_i \eta)\theta_0(\eta)_{nab} d\eta - \int_0^1 \sin(\beta_i \eta) d\eta \right] \tag{36}$$

where β_i and N_i are given by

$$\beta_i = \frac{i \cdot \pi}{2}, \quad i = 1, 2, 3... \tag{37}$$

$$\frac{1}{N_i} = \frac{2}{L} \tag{38}$$

4. RESULTS AND DISCUSSION

For the validation of the results obtained via CITT, presented in Eqs. 9 and 12, it was considered 1000 eigenvalues for the summation of the i terms. Besides, the dimensionless space position, η, was discretized for 10000 points for the simulation of its domain and the dimensionless time position, τ, was discretized for 20000 points within the range of $[0 \quad 0.2]$.

The results for the no-ablation time period, calculated by Eq. 9, are present in Fig. 3, in which the graphic on the right depicts the initial moment for the ablation time period, i.e., material is going to be expended and the boundary is expected to move along the position of the slab with an increase in the dimensionless time position.

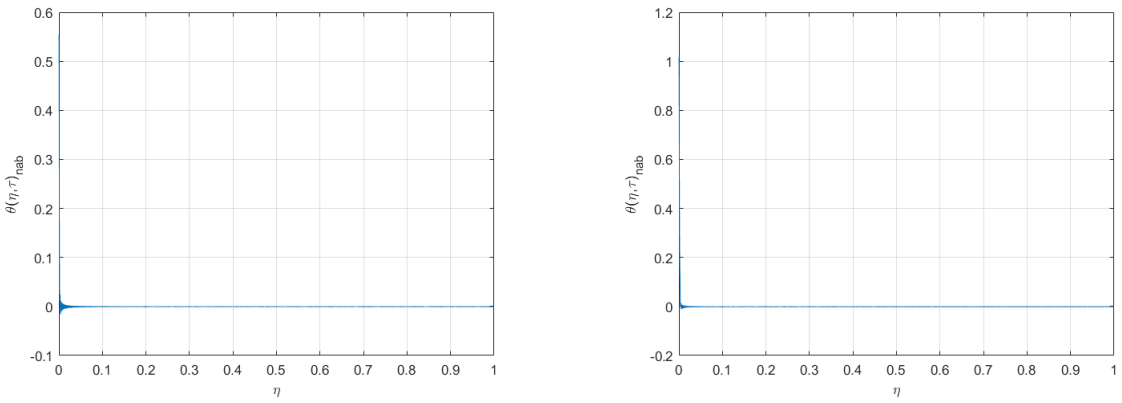

(a) $\tau = 6.0 \cdot 10^{-5}$ (b) $\tau = 1.6 \cdot 10^{-4}$

Figure 3: Temperature profile of the slab in the no-ablation time period for $\tau = 6.0 \cdot 10^{-5}$ and $1.6 \cdot 10^{-4}$.

However, Fig. 3 do not demonstrate with ease what is occurring in the temperature profile. Therefore, one need to apply a zoom in at both graphics to visualize the problem, which Eq. 9 generates (Fig. 4).

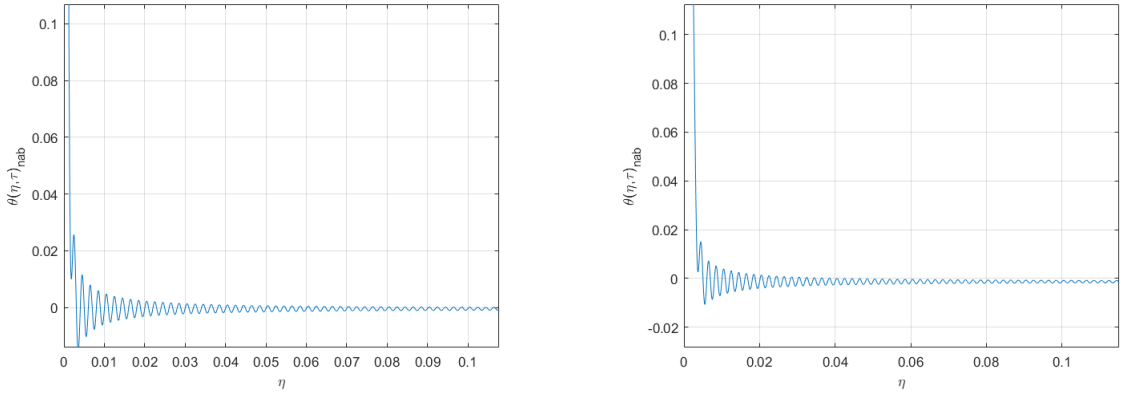

(a) $\tau = 6.0 \cdot 10^{-5}$ (b) $\tau = 1.6 \cdot 10^{-4}$

Figure 4: Temperature profile of the slab in the no-ablation time period for $\tau = 6.0 \cdot 10^{-5}$ and $1.6 \cdot 10^{-4}$.

Herein, the oscillation presented is expected to maximize the perturbation expansion for the ablation problem (Marchenko and Khruslov, 2006; Pavliotis and Stuart, 2008). This is shown in Fig. 5, with the temperature profile being computed with Eq. 12.

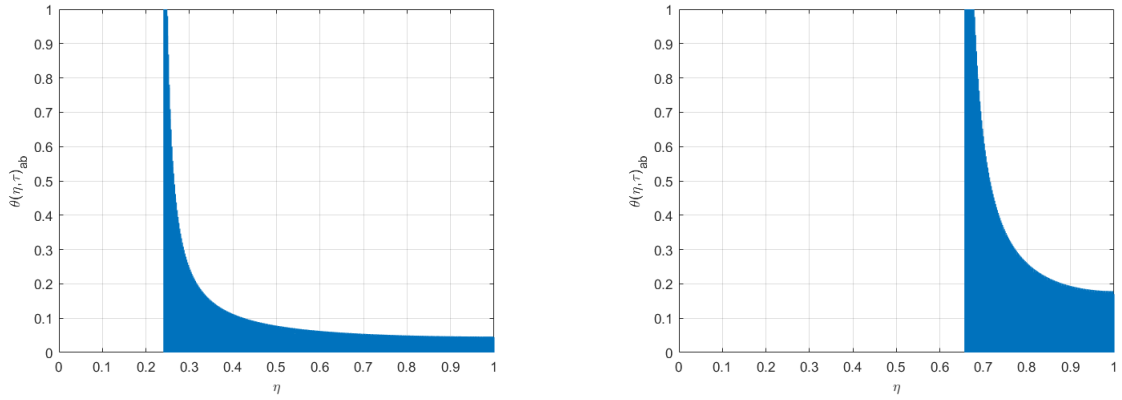

(a) $\tau = 5.6 \cdot 10^{-4}$ (b) $\tau = 9.6 \cdot 10^{-4}$

Figure 5: Temperature profile of the slab in the ablation time period for $\tau = 5.6 \cdot 10^{-4}$ and $9.6 \cdot 10^{-4}$.

As expected, the perturbation was maximized and the temperature profile could not achieve its convergence. Figure 5 represents filled curves because of the high number of eigenvalues for the summation. It is possible to note that with an increase in time, the ablative material is removed from the boundaries, from the left to the right of those graphics.

Therefore, the homogenization of the boundary conditions is considered to assess the dimensionless temperature profile and evaluate it regarding the oscillation, here presented.

For the validation of the results obtained via homogenization of the boundary conditions for CITT (Eqs. 25 and 36), it was considered 100 eigenvalues for the summation of the i terms. Besides, the dimensionless space position, η, was discretized for 1000 points for the simulation of its domain and the dimensionless time position, τ, was discretized for 5000 points within the range of $[0 \quad 0.5]$. The result for the new variables is depicted in Fig. 6

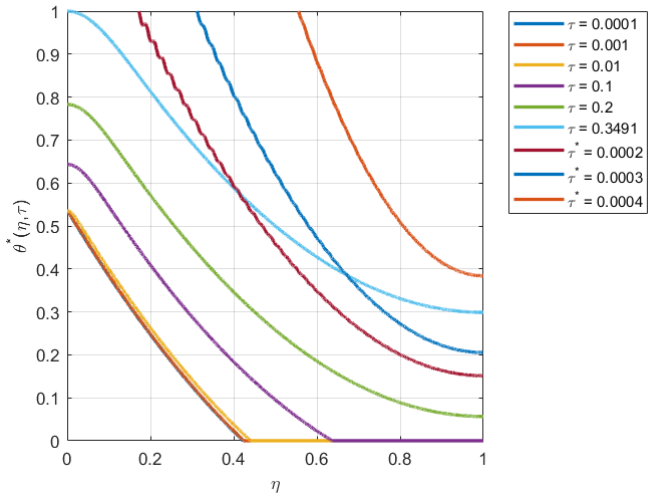

Figure 6: Temperature profile of the slab calculated via Classical Integral Transform Technique for different dimensionless time positions considering new variables which homogenize the boundary conditions.

Since the dimensionless variables developed for the homogenization of the boundary conditions contains inverted positions of η, the solution has been flipped in order to present a curve analogous to the ones seen before.

It is important to assess the no-ablation time period, represented in Fig. 6 for $\tau = 1.0 \cdot 10^{-4}$ to $3.491 \cdot 10^{-1}$, calculated by Eq. 25.

In this study, the dimensionless heat flux, $Q(\tau)$, was considered to be constant. Thus, $Q(\tau)$ = 8.05 for the TEFLON properties presented in Tab. 1. Analyzing Eq. 19, the dimensionless temperature for the non-ablation $\theta^*(\eta,\tau)_{nab}$ achieves ablation when

$$\theta^*(\eta,\tau)_{nab} = 1 + \left(\frac{1^2}{2}\right) 8.05 = 5.025 \tag{39}$$

Equation 25 calculates negative values for the temperature profile at some certain dimensionless space positions. However, it does not represent the physical problem described by the new variable. Therefore, the negative values were altered to zero.

Since the analytical result in the literature is represented for a temperature range of $[0 \quad 1]$, the temperature calculated by Eq. 25 has been normalized to fit the specified range. In addition, it is necessary to evaluate the contribution of the first eigenvalue to the dimensionless temperature profile, Eq. 27a. With the CITT approach with non-homogenized boundary conditions, the oscillation does not show the aforementioned problem, i.e., the contribution of the first eigenvalue to the summation of the i terms. Therefore, one must include the average temperature evolution (Sias *et al.*, 2007) to Eq. 25, given by

$$\theta_{av}(\tau) = \int_0^{\tau} Q(\tau')d\tau' \tag{40}$$

Thus

$$\theta^*(\eta,\tau)_{nab} = \theta_{av}(\tau) + \sum_{i=1}^{\infty} \frac{1}{N_i}\cos(\beta_i\eta)e^{(-\alpha\beta_i^2\tau)} \cdot \left[\int_0^1 \cos(\beta_i\eta)\cdot\left(\frac{\eta^2}{2}\right)\cdot Q(\tau)d\eta + \int_0^{\tau}\left(\int_0^1 \cos(\beta_i\eta)\cdot\left(\frac{\eta^2}{2}\right)\cdot\frac{dQ(\tau)}{d\tau}d\eta - \int_0^1 \cos(\beta_i\eta)\cdot Q(\tau)d\eta\right)e^{(\alpha\beta_i^2\tau)}d\tau\right] \tag{41}$$

Figure 6 presents the temperature profile in the ablation phase for $\tau^* = 2.0\cdot10^{-4}$ to $4\cdot10^{-4}$, computed with Eq. 36. From Eq. 29, the dimensionless temperature for the ablation time period $\theta^*(\eta,\tau)_{ab}$ achieves ablation when

$$\theta^*(\eta,\tau)_{nab} = 5.025 - 1 = 4.025 \tag{42}$$

Since the analytical result in the literature is represented for a temperature range of $[0 \quad 1]$, the temperature calculated by Eq. 36 has been normalized to fit the specified range.

It is important to note that an oscillation in the temperature curves for $\tau = 2.0\cdot10^{-4}$ and $3.0\cdot10^{-4}$ is present. It happens for the different range values for the dimensionless temperatures for the two distinct time periods. In other words, the phase-change in space was developed considering the last three time periods to calculate the dimensionless temperature profile for the next iteration. Thus, since the variables present different ranges for the dimensionless temperature, those time periods which present the aforementioned perturbation are neglected, for it does not represent a problem with the variable, but it is a numerical error.

Figure 7 presents the final representation for the dimensionless temperature profile with homogenized boundary conditions.

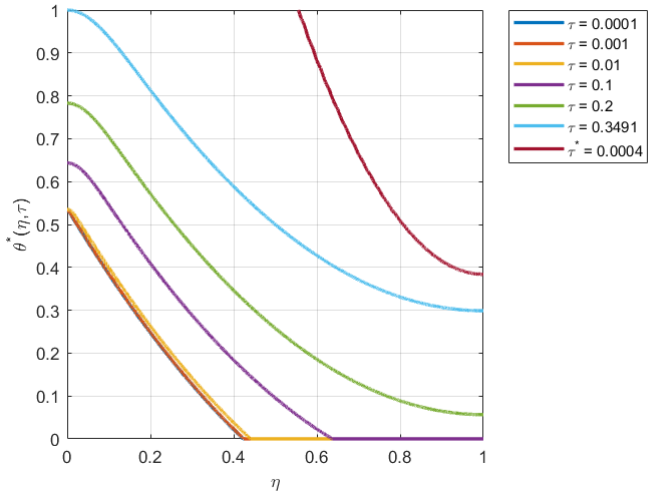

Figure 7: Final representation of the temperature profile of the slab calculated via Classical Integral Transform Technique considering new variables which homogenize the boundary conditions.

5. CONCLUSION

This study simulates the ablation phenomenon computationally, evaluating the thermal profile of the ablative material when submitted to a hypersonic external flow. The adoption of new variables for the development of an ablation study are described and elucidated, along with all the theoretical fundamentals supporting every step of the solution technique.

The study was generically developed, so one can calculate the aerodynamic heat $Q(\tau)$ and include it to the ablation phenomenon here described. Moreover, future researches could be done with a two-dimensional approach to the problem using the fundamentals here presented as a basis for the achievement of a more realistic ablation approach.

The next step of this study is the inclusion of the pyrolysis heat into the ablation phase problem. One would use the heat imposed by the external flow to chemically react ablative materials, such as graphite and glassy types of thermal protection (Diaconis *et al.*, 1961), in order to improve the ablating shield material analysis.

6. REFERENCES

Bianchi, D., 2007. *Modeling of ablation phenomena in space applications*. Ph.D. thesis, Università degli Studi di Roma "La Sapienza", Rome, Italy.

Candane, S.R., Balaji, C. and Venkateshan, S.P., 2009. "A comparison of quasi one-dimensional and two-dimensional ablation models for subliming ablators". *Heat Transfer Engineering*, Vol. 30, No. 3, p. 229–236.

Chen, N.H., 1965. "Simplified solutions for ablation in a finite slab". *American Institute of Aeronautics and Astronautics*, Vol. 3, No. 6, p. 1148–1149.

Cotta, R.M. and Mikhailov, M.D., 1993. "Integral transform method". *Applied Mathematical Modelling*, Vol. 17, p. 156 – 161.

Diaconis, N.S., Fanucci, J.B. and Sutton, G.W., 1961. "The heat protection potential of several ablation materials for satellite and ballistic re-entry into the earth's atmosphere". *Planetary and Space Science*, Vol. 4, pp. 463–478.

Gomes, F.A.A., Silva, J.B.C. and Diniz, A.J., 2005. "Radiation heat transfer with ablation in a finite plate". *Thermal Engineering*, Vol. 4, No. 2, p. 190 – 196.

Gomes, F.A.A., Silva, J.B.C. and Diniz, A.J., 2006. "Formulation of the ablation thermal problem in a unified form". *Journal of Spacecraft and Rockets*, Vol. 43, No. 1, pp. 236 – 239.

Hahn, D.W. and Özişik, M.N., 2012. *Heat Conduction*. John Wiley Sons, Inc., Hoboken, New Jersey, 3rd edition. ISBN 978-0-470-90293-6.

Marchenko, V.A. and Khruslov, E.Y., 2006. *Homogenization of Partial Differential Equations*. Birkhäuser, Boston. ISBN 978-0-8176-4468-0.

Monteiro, E.R., Macêdo, E.N., Quaresma, J.N. and Cotta, R.M., 2009. "Integral transform solution for hyperbolic heat conduction in a finite slab". *International Communications in Heat and Mass Transfer*, Vol. 36, p. 297 – 303.

Oliveira, A.P.D. and Orlande, H.R.B., 2004. "Estimation of the heat flux at the surface of ablating materials by using temperature and surface position measurements". *Inverse Problems in Science and Engineering*, Vol. 12, No. 5, p. 563 – 577.

Palaninathan, R. and Bindu, S., 2005. "Modeling of mechanical ablation in thermal protection systems". *Journal of Spacecrafts and Rockets*, Vol. 42, No. 1, p. 971–979.

Pavliotis, G.A. and Stuart, A.M., 2008. *Multiscale Methods Averaging and Homogenization*. Springer, New York. ISBN 978-0-387-73828-4.

Ruperti Jr., N.J., Cotta, R.M., Falkenberg, C.V. and Su, J., 2004. "Engineering analysis of ablative thermal protection for atmospheric reentry: Improved lumped formulations and symbolic – numerical computation". *Heat Transfer Engineering*, Vol. 25, No. 6, p. 101 – 111.

Sias, D.F., 2009. *Soluções híbridas para transferência de calor em sistemas de proteção térmica ablativos*. Ph.D. thesis, Universidade Federal do Rio de Janeiro, Rio de Janeiro, Brazil.

Sias, D.F., Ruperti Jr., N.J. and Cotta, R.M., 2007. "Enhanced convergence of integral transform solution of ablation problems". In *Proceedings of the 19th International Congress of Mechanical Engineering - COBEM 2007*. Brasília, Brazil.

Sundén, B. and Fu, J., 2017. *Heat Transfer in Aerospace Applications*. Elsevier, 1st edition. ISBN 978-0-12-809760-1.

Tannehill, J.C., Anderson, D.A. and Pletcher, R.H., 1997. *Computational Fluid Mechanics and Heat Transfer*. Taylor & Francis, Washington, DC, 2nd edition. ISBN 1-56032-046-X.